Non-linear incidental dynamics of frame structures

Goran N. Radoičić[*1], Miomir LJ. Jovanović[1a] and Dragan Z. Marinković[2b]

*[1]Department of Transport Engineering and Logistics, Faculty of Mechanical Engineering,
University of Niš, A. Medvedeva 14, Niš, Serbia*
*[2]Department of Structural Analysis, Institute of Mechanics, Berlin Institute of Technology,
Strasse des 17. Juni 135, Berlin, Germany*

Abstract.   A simulation of failures on responsible elements is only one form of the extreme structural behavior analysis. By understanding the dynamic behavior in incidental situations, it is possible to make a special structural design from the point of the largest axial force, stress and redundancy. The numerical realization of one such simulation analysis was performed using FEM in this paper. The boundary parameters of transient analysis, such as overall structural damping coefficient, load accelerations, time of load fall and internal forces in the responsible structural elements, were determined on the basis of the dynamic experimental parameters. The structure eigenfrequencies were determined in modal analysis. In the study, the basic incidental models were set. The models were identified by many years of monitoring incidental situations and the most frequent human errors in work with heavy structures. The combined load models of structure are defined in the paper since the incidents simply arise as consequences of cumulative errors and failures. A feature of a combined model is that the single incident causes the next incident (consecutive timing) as well as that other simple dynamic actions are simultaneous. The structure was observed in three typical load positions taken from the crane passport (range-load). The obtained dynamic responses indicate the degree of structural sensitivity depending on the character of incident. The dynamic coefficient K_D was adopted as a parameter for the evaluation of structural sensitivity.

Keywords: frame structure; incidental dynamics; nonlinear analysis; simulation; transient analysis

1. Introduction

Perturbations caused by external influences like wind excitation, lightning strike, overload, seismic wave, etc., lead to the appearance of extreme dynamics and large translations of big structures. The sensitivity of support structure on dynamic changes is more pronounced in the transition from working (regular) to extreme (incidental) regimes. Therefore, the modern structural design is more and more directed to the dynamic stability at extreme incidental events.

There are heavy frame structures on big cranes. The jib support tie rod is a high loaded structural part where a fracture (disruption) occurs most often. Will the local fracture jeopardize

---

∗Corresponding author, M.Sc., E-mail: goran.radoicic@jkpmediana.rs
[a]Professor, E-mail: miomir@masfak.ni.ac.rs
[b]Ph.D., E-mail: Dragan.Marinkovic@TU-Berlin.de

the structural stability? Will the redundancy enable the stability preservation? The simulations of extreme transient regimes give the responses to these questions.

Practical examples on the crane structures indicate simultaneous appearance of incidents (a single incident causes the next incident), after which the large amplitudes of vibration and the structural damages result. The subject of a possible design then is a structure with still preserved global stability. The mechanism of the whole structure overturn is not a subject of simple incidents, and it is often the consequence of the actions for which structures are not prepared (such as tsunami, tectonic movement, fall of an adjacent object on the structure, etc.).

Discrete incidental situations can cause local damages but they can also pass without them. A discrete incident arises more often in practice by the load management error with the simultaneous failure (fracture) of some responsible element, usually a connection element. Accordingly, two incidents are discussed. That is when the uncontrolled load sway occurs, as well as the disconnection between a counter-jib support tie rod and the hoisting jib. The second incidental combination of structural load is often caused by overload. The combination of effects causes unexpected, often intensive dynamics.

Isherwood (2010) provided an insight into the global presence of incidents on structures. Incidents are a real danger because at least one incident for each manufacturing brand of crane, according to Isherwood (2010), has been recorded.

Structural analysts, in recent studies, consider various cases of failures and the non-functional consequences of structural components caused by fracture and other incidental influences. Also, very topical is application of numerical simulations to study the dynamic behavior of frame structures as well as application of geometrically nonlinear analyzes. For example, the influence of wind excitation, as a potentially extreme (incidental) dynamical influence, on large truss tower structures was considered by Qu *et al.* (2001) using an analytical method for determining dynamic response which was based on the numerical integration of equations of motion for the two finite element models (static and dynamic). Cho *et al.* (2012) considered the wave-induced excitation as a serious dynamic perturbation which could jeopardize the dynamic stability of see-floating port or mobile harbor with a large-scale heavy crane system. Ibrahim *et al.* (2013) investigated the effects of crack location and crack depth on free vibration of cracked frame structures using the FEM model with a crack element that was developed on the fracture mechanics principles. Katkhuda *et al.* (2010) showed a novel system for damage detection at the local element level under normal operating conditions and structural health assessment of steel frame structures. Shi *et al.* (2008) developed a numerical model to simulate and analyze the dynamical behavior of different types of steel connection between the structural elements achieved by using the bolted end-plates. Da Silva *et al.* (2008) included the geometrical non-linearity in their modeling strategy of the dynamical behavior of frame structures under dynamic actions using the finite element analysis. Kettal and Wiberg (2004) indicated that the simulation of failure process is an inherently difficult task because it includes solving of a large set of nonlinear equations which require use of newer and faster numerical methods for structural mechanics applications.

2. Geometrically nonlinear transient dynamics

Structural analysts tend to employ linear models and analysis whenever this allows a sufficiently accurate approximation of the actual structural behavior. The prediction of linearity of the structural response rests however on certain assumptions, such as rather small displacements

compared to the dimensions of the modeled structure, linear elastic material behavior as well as unchangeable boundary conditions during the analysis.

Geometrically-only nonlinear structural analysis is characterized by non-negligible changes in structural configuration, whereas the induced strains and stresses remain within the realm of material linear behavior. While the structural behavior of a tower crane in most typical working conditions can be described with sufficient accuracy by a linear model, this paper considers a case of incident involving structural behavior that is beyond the limit of geometrical linearity. Hence, the conducted analysis is of geometrically nonlinear type.

The FEM equation of geometrically nonlinear transient structural dynamics, at the time t, has the following form

$$[M]^t\{\ddot{u}\} + {}^t[C]^t\{\dot{u}\} = {}^t\{f_{ext}\} - {}^t\{f_{\mathbf{int}}\}$$ (1)

where $[M]$ and $[C]$ are the mass and damping matrices, $\{f_{ext}\}$ and $\{f_{int}\}$ are the external (excitation) and internal (elastic) forces of the FEM assemblage, $\{u\}$ are the structural displacements with dots above denoting time derivatives (acceleration and velocity), while the left superscript denotes at which moment of time the quantity is taken. The geometrically nonlinear analysis requires computation of engineering stresses in the current structural configuration, $\{\sigma\}$, and their integration over the current structural domain, ${}^tV$, in order to obtain the internal structural forces

$$^t\left\{f_{\mathbf{int}}\right\} = \int\limits_{{}^tV} {}^t[B]^t\{\sigma\}d\,{}^tV$$ (2)

where $[B]$ is the strain-displacement matrix (yielding the linear part of the strain field) of the FE assemblage.

The integration of dynamic equilibrium Eq. (1) is the most time-consuming part of the FEM transient computation. Geometrically nonlinear analysis requires direct integration methods, which are divided into the group of explicit methods and group of implicit methods. The main differences between them are the expense of calculating one time step, the time step size due to stability criteria and at which moment of time the equilibrium is considered.

The equilibrium at time t (Eq. (1)) is suitable for the time-marching-forward schemes of explicit methods. They are rather inexpensive regarding the computational effort required to compute a single time step. However, the size of the time step is restricted and has to be smaller than a certain critical value for the solution to be stable. The critical time step directly depends on the largest eigenfrequency of the finite element assemblage influenced by the discretization of the structure. Another consequence of a short time step is that the iteration errors due to nonlinearities are negligible and hence, no iterations are performed.

The implicit methods are unconditionally stable, which accounts for their advantage. However, the time step is certainly limited by the required level of accuracy. More precisely, it depends on the highest eigenfrequency in the structural response that is of interest for the analysis. A general recommendation is to choose the time step size so as to split the period of the highest eigenfrequency of interest into 8-10 segments. It should also be taken into account that, within an implicitly integrated geometrically nonlinear transient analysis, large time steps imply a relatively large computational effort to resolve a time step due to the coupled system of equations and necessary iterations.

Finally, to resolve the structural configuration at time $t+\Delta t$, the equilibrium equation for the very same moment in time (i.e., $t+\Delta t$) is used.

The structure considered in the paper is made of steel and the conditional stability of an explicit time integration would impose a critical time step of the order of magnitude of $10^{-7} \div 10^{-5}$ s. Taking additionally into account the considered excitation and the range of structural vibration modes that is of interest, a reasonable choice would be an implicit time integration scheme with a time step of 10^{-3} s. Such a choice also filters out effectively higher modes in the structural response. The choice of the authors is the Newmark time integration. The system of equations for geometrically nonlinear structural dynamics for time $t+\Delta t$ reads

$$[M]^{t+\Delta t}\{\ddot{u}\}^{(k)} + {}^{t+\Delta t}[C]^{t+\Delta t}\{\dot{u}\}^{(k)} + {}^{t+\Delta t}[K_T]^{t+\Delta t}\{\Delta u\}^{(k)} = {}^{t+\Delta t}\{f_{ext}\} - {}^{t+\Delta t}\{f_{\mathbf{int}}\}^{(k-1)} \tag{3}$$

where $[K_T]$ is the tangential stiffness matrix, Δ denotes the increment of a quantity and k denotes the iteration. The tangential stiffness matrix together with the increment of displacements enables estimation of the internal forces at time $t+\Delta t$. According to the updated Lagrangian formulation, the tangential stiffness matrix is computed as

$$^t[K_T] = {}^t[K_L] + {}^t[K_\sigma] \tag{4}$$

where ${}^t[K_L]$ is the linear stiffness matrix and ${}^t[K_\sigma]$ is the geometric stiffness matrix, both determined for the current structural configuration, i.e., at time t as

$$^t[K_L] = \int_{{}^tV} {}^t[B]^{\mathrm{T}}[H]^t[B] \, d^tV \tag{5}$$

$$^t[K_\sigma] = \int_{{}^tV} {}^t[B_{NL}]^{\mathrm{T}} {}^t[\sigma]^t[B_{NL}] \, d^tV \tag{6}$$

where $[H]$ is the Hooke's matrix, $[B_{NL}]$ is the matrix that yields the nonlinear part of the strains and $[\sigma]$ is the stress state given in matrix form, all of them defined at the current structural configuration, i.e., at time t.

Within the Newmark integration method, the following assumptions are employed

$$^{t+\Delta t}\{u\} = {}^t\{u\} + \frac{\Delta t}{2}\left({}^t\{\dot{u}\} + {}^{t+\Delta t}\{\dot{u}\}\right) \tag{7}$$

$$^{t+\Delta t}\{\dot{u}\} = {}^t\{\dot{u}\} + \frac{\Delta t}{2}\left({}^t\{\ddot{u}\} + {}^{t+\Delta t}\{\ddot{u}\}\right) \tag{8}$$

and, additionally, the incremental relation yields

$$^{t+\Delta t}\{u\}^{(k)} = {}^{t+\Delta t}\{u\}^{(k-1)} + \{\Delta u\}^{(k)} \tag{9}$$

Introducing Eqs. (7)-(9) into Eq. (3), one obtains

$$^t[\hat{K}]\{\Delta u\}^{(k)} = {}^{t+\Delta t}\{f_{ext}\} - {}^{t+\Delta t}\{f_{\mathbf{int}}\}^{(k-1)} - [M]\left(\frac{4}{\Delta t^2}\left({}^{t+\Delta t}\{u\}^{(k-1)} - {}^t\{u\}\right) - \frac{4}{\Delta t}{}^t\{\dot{u}\} - {}^t\{\ddot{u}\}\right) -$$
$$-[C]\left(\frac{2}{\Delta t}\left({}^{t+\Delta t}\{u\}^{(k-1)} - {}^t\{u\}\right) - {}^t\{\dot{u}\}\right) \tag{10}$$
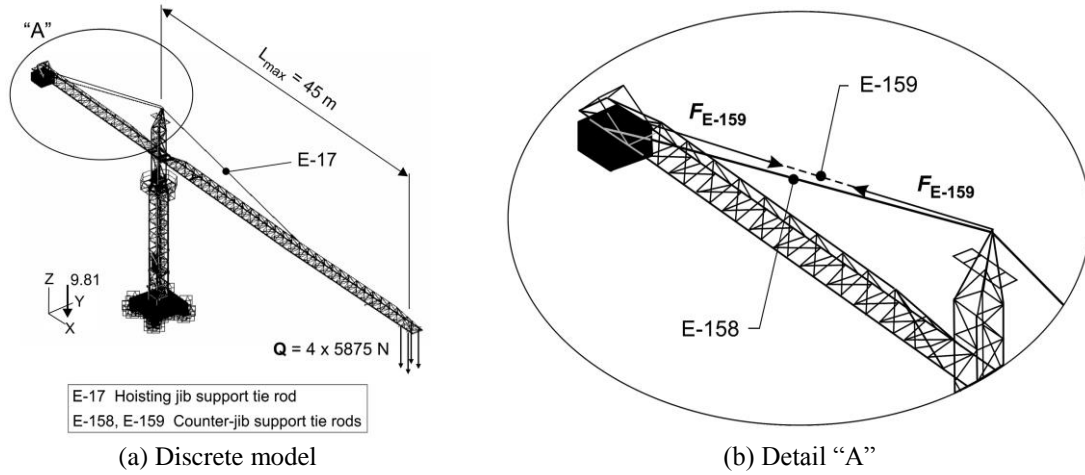
with the system matrix $[\hat{K}]$ given as

(a) Discrete model   (b) Detail "A"

Fig. 1 Tower crane POTAIN 744E

$$ {}^t\left[\hat{K}\right] = {}^t\left[K\right] + \frac{2}{\Delta t}\,{}^t\left[C\right] + \frac{4}{\Delta t^2}\left[M\right] $$ (11)

The discrete tower crane model POTAIN 744E (hereinafter: TC), shown in Fig. 1(a), and its detail "A", shown in Fig. 1(b), illustrate the extreme dynamics research of the structure. The precise introduction of the concentrated masses in the model leads to quality improvement - to the accuracy of a solution (Jovanović *et al.* 2011). The developed theoretic model TC was based on beam and rod elements (MSC NASTRAN). To describe the crane foundation of reinforced concrete, the 8-node solid element is used. The developed model of the tower crane structure is characterized by mass M_M=72204 kg, number of finite elements N_E=1667, number of nodes N_N=1146 and total DOF number N_{DOF}=6876.

In the direct transient analysis, the experimentally identified overall structural damping coefficient G=0.05 by Radoičić and Jovanović (2013) was used. The conversion of overall structural damping G and element structural damping G_E into an equivalent viscous damping using the model MSC and Eq. (12) by Rose (2002) and the dominant circular frequencies ω_3 and ω_4 from the modal analysis (Jovanović *et al.* 2011), was performed by Radoičić and Jovanović (2013). Eq. (12) contains: [C] complex damping matrix, [C_V] viscous damping matrix, [K] global stiffness matrix and [K_E] element stiffness matrix.

$$ \left[C\right] = \left[C_V\right] + \frac{G}{\omega_3}\left[K\right] + \frac{1}{\omega_4}\sum G_E\left[K_E\right] $$ (12)

3. Experimental basis of the research

Basic characteristics of the investigated TC are: range of 45 m, total height of 23.5 m, hoisting height of 16 m and maximal carrying capacity of 10 t at reach of 14.8 m. Under the working load, the vertical vibrations of the concrete foundation were very small. The highest vertical displacement of the foundation amounted to 4/100 mm (see Fig. 2(a)). The experimental

(a) Foundation deflection   (b) Force on hook and acceleration   (c) Micro-deformations of tie rod
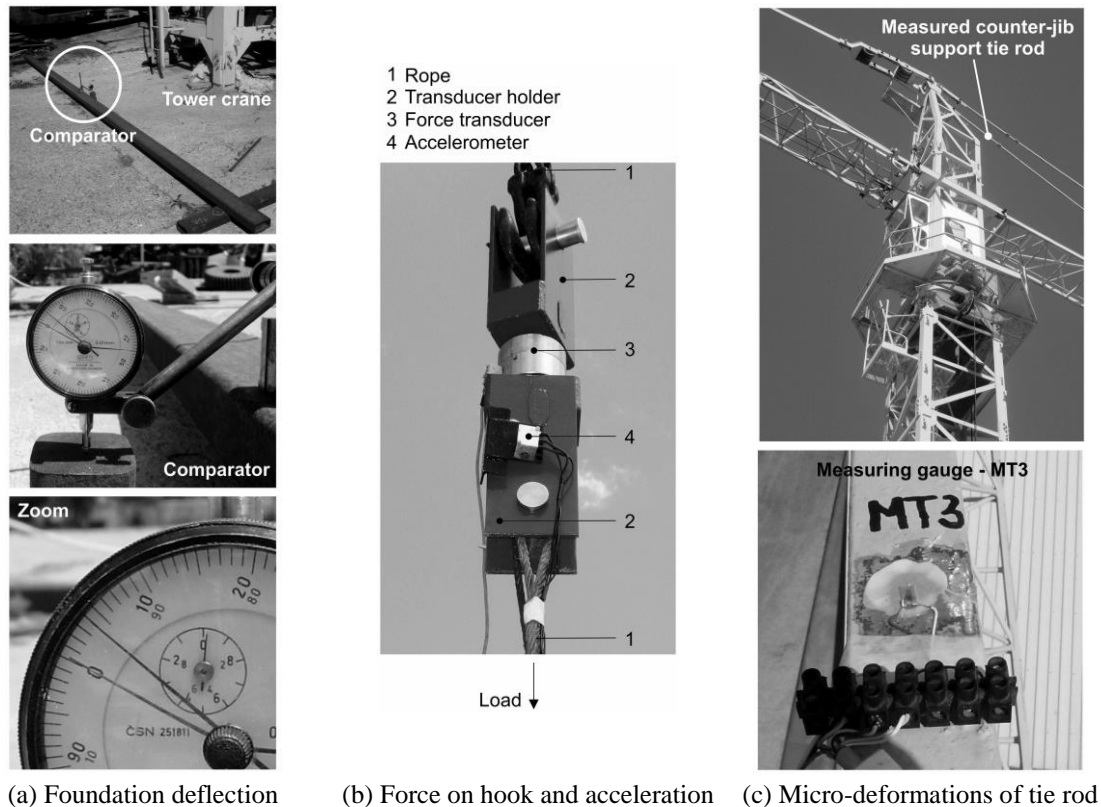
Fig. 2 Experimental measurements of the tower crane POTAIN 744E

measurement of foundation deflection was performed using the measuring system shown in Fig. 2(a) (Jovanović *et al.* 2012b). Incidental dynamics research requires the determination of several experimental values such as: unload time of hoisting rope, unload time of a counter-jib support tie rod (due to fracture) and axial force in the remaining counter-jib support tie rod. Fig. 2(b) shows a part of the measuring system to determine the force on the hoisting rope and the acceleration of load. Fig. 2(c) shows the position of the measuring point MT3 on the TC, to measure the micro-deformations of a counter-jib support tie rod.

From the diagram in Fig. 3 the unload time of structure Δt_I caused by the load fall was obtained, i.e., $\Delta t_I = t_4 - t_3 = 0.83$ s. The trial load of mass $m = 2.2$ t at maximum range $L_{\max}$ and a force transducer shown in Fig. 2(b), in the experiment were used. The HBM measuring equipment and HBM CatMAN AP software were used for measurement and processing of results.

The interruption of the connection between a counter-jib support tie rod and rest of the crane structure was caused by an extremely strong strike of the load to the ground. Therefore, the duration of interruption by short time of creation less than the duration of load striking the ground was defined. Such choice of incidental time corresponds to destruction or disconnection. The time of the tie rod interruption Δt_F was empirically adopted, i.e., $\Delta t_F = 0.6$ s $< \Delta t_I = 0.83$ s.

Using the measuring gauge MT3 placed on the counter-jib support tie rod (see Fig. 2(c)), the deformations caused by the examination regimes were measured. The experimental excitation was caused by hoisting and suddenly lowering the load until striking the ground. The experimental idea
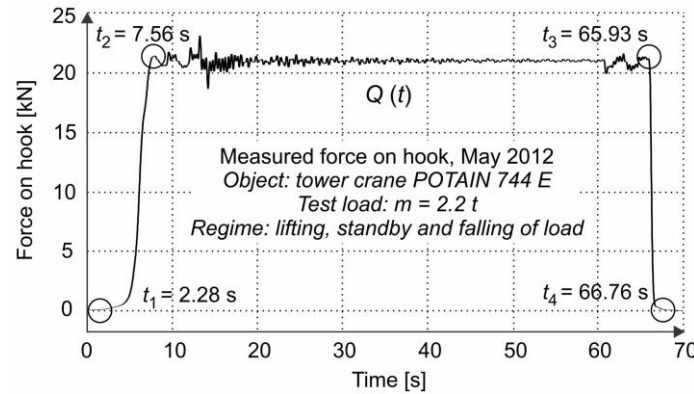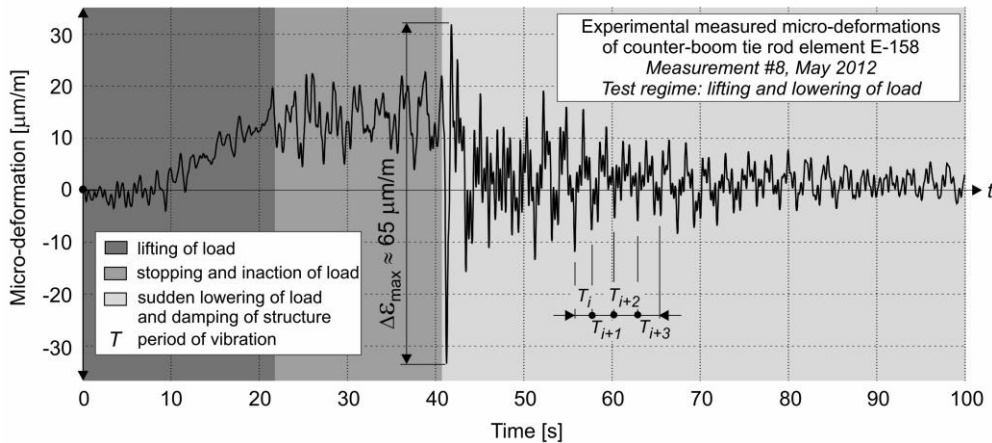
Fig. 3 Record of the measured force on hook

Fig. 4 Record of the measured deformations by measuring gauge MT3

included the determination of deformation values shown in Fig. 4, and then the computation of all total changes of axial force in the counter-jib support tie rod in the duration of simulation. Although a support tie rod was not physically interrupted in the experiment, this measurement was useful to inform us about the real forces in the counter-jib support tie rod.

On the basis of the experimentally measured deformation ε_i, the axial force F_i is computed (the Hooke's law). Thus obtained, the experimental values of force F_i are enlarged by adding the value of the static axial force in the tie rod. The measurement did not include this static force. The measuring regime was different than the simulation regime because the mechanical interruption - fracture of a tie rod element was not caused experimentally. The largest measured value of the change of micro-deformation was extracted as $\Delta\varepsilon_{max} \approx 65$ μm/m. This value corresponds to the largest change of the axial force $\Delta F_{E\text{-}158,max} \approx 77$ kN in the element E-158.

4. Incidental effect models

The basic models of incidental effects are shown in Fig. 5 using the approximate perturbation
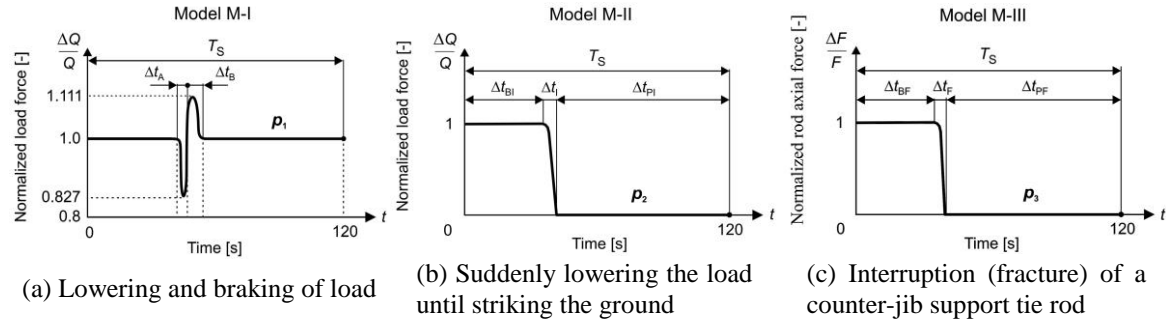
(a) Lowering and braking of load   (b) Suddenly lowering the load   (c) Interruption (fracture) of a
                                    until striking the ground   counter-jib support tie rod

Fig. 5 Three basic incident load models

function p_i (i=1, 2, 3). Actually, this function is the change of normalized load force in time for models M-I and M-II contrary to the model M-III where the function is displayed as the normalized rod axial force. The normalization was performed according to the static value of load force and rod axial force.

The approximate function p_1 of the model M-I has the impulse form corresponding to the rapid lowering and the following sudden braking of the load Q before striking the ground (see Fig. 5(a)). The model M-I is the very frequent effect case in the practical handling of load, according to Radoičić and Jovanović (2012).

The effect model M-II, shown in Fig. 5(b), corresponds to the rapid lowering of load until striking the ground. The duration of unloading is taken from the experiment and it is Δt_I=0.83 s (see Fig. 3). The model is introduced by the normalized load force $\Delta Q/Q$ (Radoičić *et al.* 2011) i.e., the perturbation function p_2.

The third basic model of the incidental effect M-III is similar in its form to the previous model, except that the function p_3 relates to the internal - axial force of a counter-jib tie rod and it represents the normalized force $\Delta F/F$ (see Fig. 5(c)). In this model, an interruption of physical connection between a counter-jib tie rod and tower occurs in one moment. This sudden change is a consequence of the fallout of a pin for the tower-rod connection. The interruption can also be a consequence of the random collision of two cranes with the damage of fracture. The duration of the static force change in the tie rod is a short-term for all processes with the discontinuation of kinematic coupling, so the unload time in the tie rod is estimated according to the experimentally measured duration of the structure unloading. Considering the smaller mass and energy of the tie rod, the slightly shorter duration of the effect change (fracture) of Δt_F=0.6 s was approximately determined by Jovanović *et al.* 2012a.

Fig. 5 uses the following labels: Δt_A is the acceleration time, Δt_B the braking time, Δt_{BI} the time before incident, Δt_I the incident time of load, Δt_{PI} the calming time of structure, Δt_{BF} the time before fracture, Δt_F the fracture time, Δt_{PF} the post fracture time and T_S = 120 s is the simulation time. The acceleration time Δt_A and the braking time Δt_B were determined by Radoičić and Jovanović (2012) when solving the dynamic model of hoisting mechanism.

5. Simulation scenarios

Experimental dynamic investigation is a risky job because the structural stability is often

Scenario S-I.1 — (a) First combination of models M-I (function p_1) and M-III (p_3)

	t_0	t_1	t_2	t_3	t_4	t_5	t_6	t_7
t_i [s]	0	40.25	40.36	40.45	40.59	40.75	41.35	120
p_1 [-]	1	1	0.827	1	1.111	1		1
p_3 [-]	1	1				1	0	0

Scenario S-I.2 — (b) Second combination of models M-I (p_1) and M-III (p_3)

	t_0	t_1	t_2	t_3	t_4	t_5	t_6	t_7	t_8
t_i [s]	0	40	40.25	40.36	40.45	40.59	40.6	40.75	120
p_1 [-]	1		1	0.827	1	1.111		1	1
p_3 [-]	1	1					0		0

Scenario S-II.1 — (c) Combination of models M-II (p_2) and M-III (p_3)

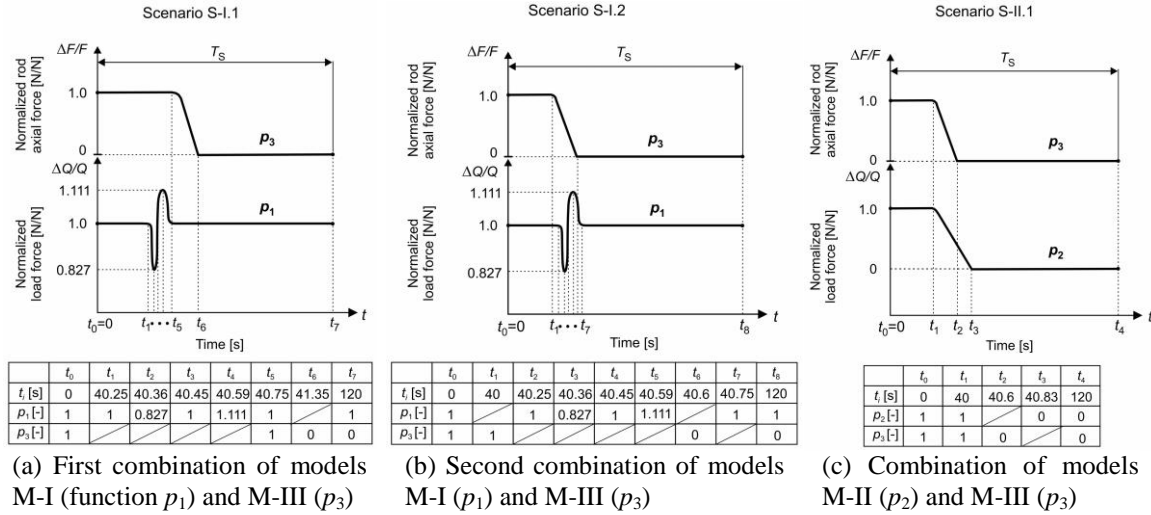|	t_0	t_1	t_2	t_3	t_4
t_i [s]	0	40	40.6	40.83	120
p_2 [-]	1	1		0	0
p_3 [-]	1	1	0		0

Fig. 6 Incidental combinations of the basic models

endangered. Therefore, simulation methods are alternatively applied. The simulation scenarios are the ways for introduction of individual effects to the load process. Scenarios determine the time impact of excitation and they describe the extreme dynamic regimes. Scenarios also contain the incidental extensions as the consequences of the previous failures (incidental combinations). In each of the situations in Fig. 6, a failure of a counter-jib support tie rod is simulated. Thus, the tie rod axial force is excluded from the static balance of the support structure. Such sudden event causes the dynamic increase (reallocation) of internal forces in a structure.

The incidental scenario **S-I.1** in Fig. 6(a) is characterized by consecutive perturbation and an algorithm in which: the crane operator begins the sudden lowering of load at the velocity of v=20 m/min at the moment t_1=40.25 s (curve p_1, acceleration period t_3–t_1=0.2 s); then the operator stops the load until the moment t_5=40.75 s (curve p_1, braking period t_5–t_3=0.3 s); a fracture of one counter-jib support tie rod then occurs as a consequence of the previous effect at the moment t_5=40.75 s, while the unloading lasts for Δt_F=0.6 s (curve p_3, t_6–t_5); the total interruption of the tie rod occurs at the moment t_6=41.35 s; the damping vibration of the structure (calming) lasts until the end of simulation t_7=120 s (curves p_1 and p_3).

The simulation model **S-I.2** in Fig. 6(b) represents the simultaneity of two perturbations and takes place according to the following scenario: the earlier damages in the material of joint connections at one counter-jib tie rod (curve p_3, t_1=40 s) lead at a moment to the interruption of the tie rod (curve p_3, t_6=40.6 s); not understanding the failure of this responsible element, the crane operator at the moment t_2=40.25 s (curve p_1) starts the extreme rapid load lowering at the velocity of v=20 m/min; the acceleration period is t_4–t_2=0.2 s (curve p_1); the operator then extremely suddenly stops the load by braking at the moment t_7=40.75 s (curve p_1, braking period t_7–t_4=0.3 s); the damping vibration of structure lasts until the end of simulation i.e., t_8=120 s (curves p_1 and p_3).

Finally, the incidental dynamic simulation of the load fall, denoted as **S-II.1** in Fig. 6(c), is performed according to the scenario: the previous damages in the linkage system of counter-jib and tower cause the fracture of one tie rod (curve p_3, t_1=40 s); simultaneously, the sudden lowering of load starts with the interruption of the tie rod (curve p_2, t_1=40 s); the fracture of the tie rod lasts until the moment t_2=40.6 s (curve p_1); after the rapid lowering, it comes to load striking the ground

Table 1 Dynamic responses of the modeled structural configuration

Element	Carrying capacity t	$F_S{}^*$ [N]			$F_{D,\max}{}^*$ [N]			$K_D{}^* = F_{D,\max} / F_S$ [-]		
		Incidental scenario								
		S-I.1	S-I.2	S-II	S-I.1	S-I.2	S-II.1	S-I.1	S-I.2	S-II.1
E-17	10	337814	533416	282099	362546	578766	352714	1.073	1.085	1.250
	2.9	474476	474481	293474	503397	516603	353626	1.061	1.089	1.205
	2.35	466471	455634	293887	496471	501908	351655	1.064	1.102	1.197
E-158	10	439788	439843	439572	476301	481482	568992	1.083	1.095	1.294
	2.9	439849	439871	440155	475813	476726	547066	1.082	1.084	1.243
	2.35	439691	439854	439897	478679	477844	543192	1.089	1.086	1.235

$^*F_S$: Static force; $F_{D,\max}$: Max dynamic force; K_D: Dynamic coefficient

at the moment t_3=40.83 s (curve p_3) when the structural unloading arises and it lasts for Δt_I=0.83 s (experimentally measured); the damping of structure takes place in the end of simulation and it lasts until the moment t_4=120 s (curves p_2 and p_3).

6. Analysis of simulation results

The results of analyses gave the dynamic responses (axial forces and dynamic coefficients) for two responsible structural elements, the hoisting jib support tie rod (Element E-17) and the counter-jib support tie rod (Element E-158). The dynamic responses are shown in Table 1.

Three characteristic carrying capacities (working points) for analysis are selected from the crane passport: a. 10 t at 14.8 m of reach, b. 2.9 t at 39 m and c. 2.35 t at 45 m. This choice of carrying capacities included the extreme permissible load of burden (a.), the maximal reach (c.) and the position (b.) of the highest dynamic coefficient according to Jovanović *et al.* (2012a). For the evaluation of structural sensitivity on incidental dynamics the dynamic coefficient K_D is adopted. It is the ratio of the maximal dynamic force $F_{D,\max}$ and the static force F_S in the same element after an incident (see Eq. (13)).

$$K_D = \frac{F_{D,\mathbf{max}}}{F_S} \qquad (13)$$

6.1 Case studies S-I.1 & S-I.2

The simulation of the incidental scenario S-I.1 (acceleration–braking & fracture) first was performed. Thus, the dynamic records of force in the hoisting jib support tie rod (Element-17) for three selected carrying capacities have been obtained and shown in Fig. 7(a). The diagram in Fig. 7(a) shows higher values of the axial force under the load m=2.9 t at the reach L=39 m, especially of the maximal dynamic force $F_{D,\max}$ and the post-incident (static) force $F_{St\text{-}PI}$. After the structure calming, the post-incident axial forces in the element E-17 at all carrying capacities in Fig. 7(a), returned to own values as before the incident i.e., $F_{St\text{-}PI} \cong F_{BI}$.

Fig. 7(b) shows the change of axial force in the remaining counter-jib support tie rod E-158 obtained according to the scenario S-I.1. Since the similarity of the obtained dynamic responses in

(a) Axial forces in the hoisting jib support tie rod E-17 for three carrying capacities

(b) Axial force in the counter-jib support tie rod E-158 for the longest boom range
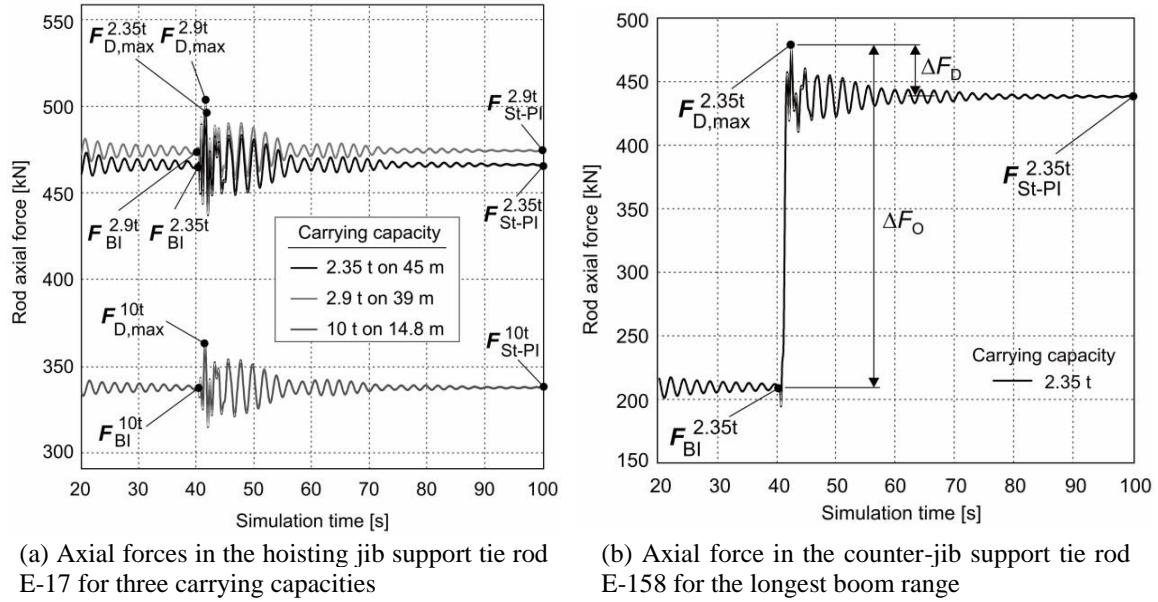
Fig. 7 Scenario S-I.1, axial forces

the three capacity-range cases existed, only one curve of the axial force in the element E-158 for the capacity of 2.35 t at reach of 45 m here is shown. The dynamic response in Fig. 7(b) gives the insight into one more dynamic parameter. It is about the coefficient of overall force growth K_F. Actually, this coefficient is the ratio of the maximal dynamic force $F_{D,max}$ and the before-incident axial force F_{BI} in a selected element (see Eq. (14)). The coefficient K_F indicates the new equilibrium situation of a structure and local reallocation of forces after an incident (redundancy).

$$K_F = \frac{F_{D,\mathbf{max}}}{F_{BI}}. \tag{14}$$

Using Eq. (14) and the force values $F_{D,max}$ and F_{BI}, indicated in Fig. 7(b), the coefficient of overall force growth of the remaining counter-jib support tie rod E-158 in the simulation S-I.1 was calculated. This coefficient took a very high value of K_F=2.28. The labels in Fig. 7(b) are: ΔF_O is the overall force growth (jump) and ΔF_D is the highest force change at modified geometry under an incident.

The calculated stresses in all incidental combinations with the interruption of a support tie rod took values which ranged within the area of permissible static stress for the constructive steel from the group I.

According to the scenario S-I.2, the changes of axial forces in the jib tie rods were very similar to the situations in the scenario S-I.1 from Fig. 7, so they were not shown especially. Only in the case S-I.2, the dynamic coefficients were more pronounced at higher carrying capacities.

6.2 Case study S-II.1

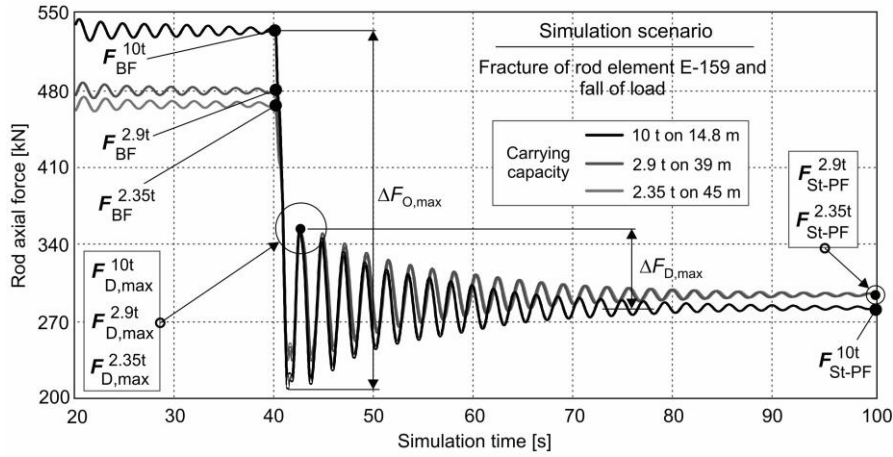After the combined incidental effect, according to the scenario S-II.1, the different values of

Fig. 8 Scenario S-II.1, axial forces in the hoisting jib support tie rod E-17 for three carrying capacities
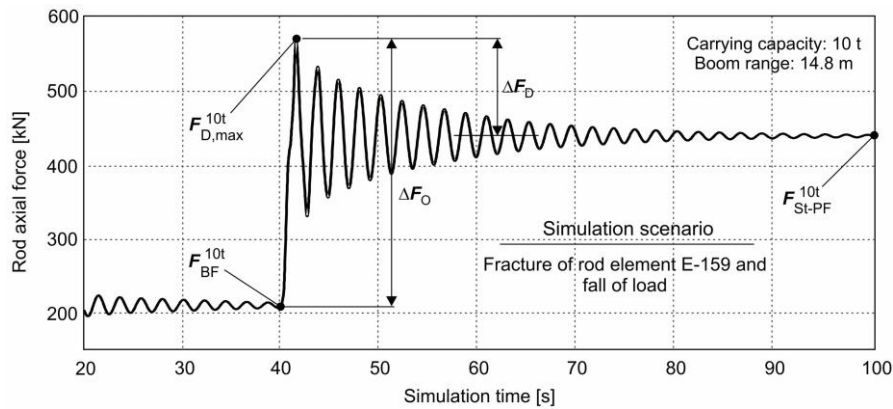

Fig. 9 Scenario S-II.1, axial force in the counter-jib support tie rod E-158 for the capacity of 10 tons

internal dynamic forces in the tie rod E-17, at different carrying capacities, can be practically observed only in the second part of simulation (see Fig. 8). The indicator of these differences is the internal dynamic force $F_{St\text{-}PF}$. In an area of the diagram after the incident $t>40.83$ s, it applies

$$F_{St-PF}^{2.9t} \cong F_{St-PF}^{2.35t} \neq F_{St-PF}^{10t} \tag{15}$$

The diagrams of axial force in the counter-jib tie rod E-158 for different carrying capacities are very similar so they can be replaced with one, e.g. the diagram for the carrying capacity of 10 t on the reach of 14.8 m (see Fig. 9). The intensity of maximal dynamic force $F_{D,\max}$ was more pronounced than in the previous scenarios.

The dynamic coefficients K_D were higher by up to 20% in the simulation case S-II.1 in relation to the previous scenarios (see Table 1). It indicates that the incidental scenario S-II.1 was the unfavourable scenario with the aspect of geometric sensitivity in relation to the dynamic structural changes. Also, the largest vertical translation was found in the S-II.1 scenario.

Fig. 10 shows the total translations of the end node N-1409 of hoisting jib under the load of mass m=10 t at the reach L=14.8 m. This load/reach corresponds to higher dynamic coefficients of
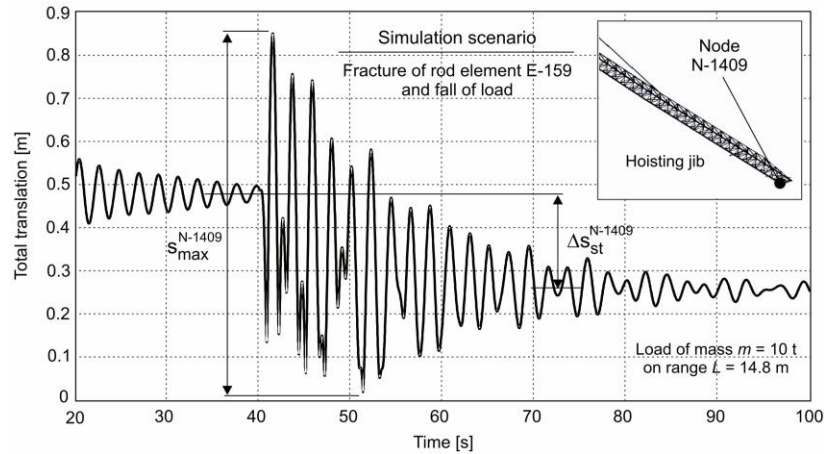
Fig. 10 Scenario S-II.1, total translations of the node N-1409 (dominantly vertical movement)
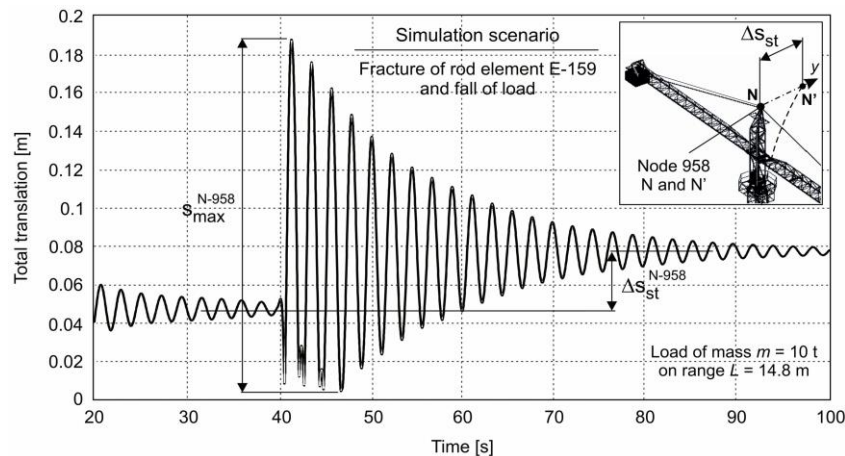

Fig. 11 Scenario S-II.1, total translations of the node N-958 (dominantly lateral movement)

the hoisting jib tie rod and the counter-jib tie rod shown in Table 1. The dominant direction of translation is the vertical direction. The largest translation was caused by incidental dynamics in the node N-1409. This translation took the value S_{max}(N-1409)=0.84 m (see Fig. 10), while the difference of static deflection, prior and after the interruption of a counter-jib support tie rod and the sudden unloading, took the value ΔS_{st}(N-1409)=0.22 m. The translations of the end node of hoisting jib can be larger in cases of overload at the maximal range.

The lateral translation of the tower top caused by the interruption of a support tie rod was not large and the largest amounted S_{max}(N-958)=0.18 m (see Fig. 11). The lateral translation of the tower top after the incident and structural calming due to the disturbed geometrical symmetry amounted ΔS_{st}(N-958)=0.03 m.

6.3 Dynamic coefficients

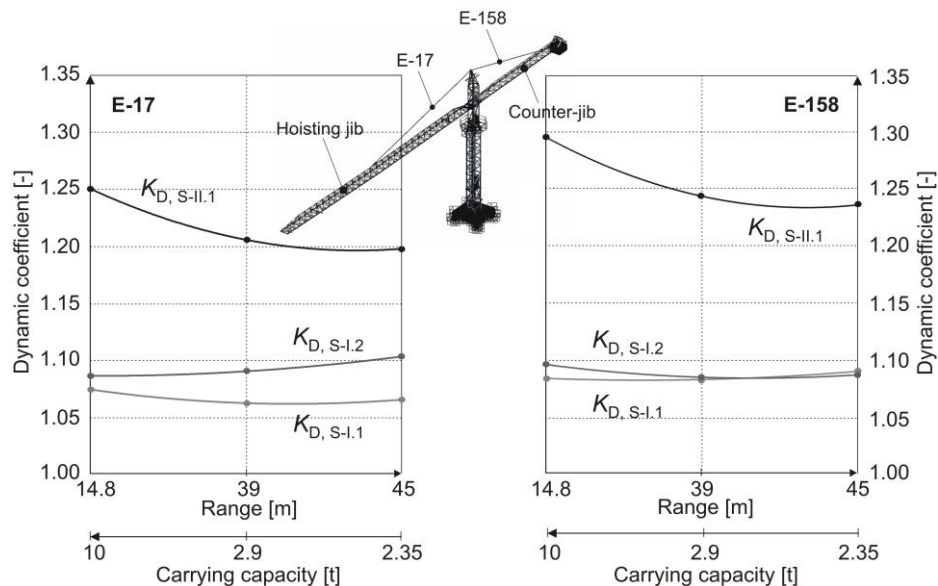The diagrams in Fig. 12 show the dynamic coefficients K_D for two selected responsible

Fig. 12 Dynamic coefficients K_D for the hoisting jib tie rod (left) and the counter-jib tie rod (right)

structural elements, E-17 and E-158. The coefficients K_D were obtained by simulation of three incidental scenarios with combined loads. The range of corresponding carrying capacities on the abscissa of the diagrams is shown, and the values of the coefficient K_D on the ordinate are shown.

The greatest dynamic changes are caused by the incidental effect S-II.1 (tie rod fracture and load striking the ground) at all load ranges. This is shown in Fig. 12 by the curve $K_{D,S-II.1}$. The regime S-I.2 followed in the case of the hoisting jib support tie rod E-17 as well as the counter-jib support tie rod E-158 only for bigger loads at shorter ranges. Dynamics of the regime S-I.1 exerted least influence on the structure. Comparing the two responsible elements, one can see that the counter-jib tie rod E-158 generally has higher sensitivity on incidental dynamics in 78% of the observed combined loads.

7. Conclusions

• The developed FEM model of a structure of heavy lifting and moving machinery is experimentally and numerically verified. This model is proposed for use due to its completeness and small geometric approximations. The model introduces even very small constructive elements and, accordingly, faithfully represents the real structure.

• The composed FEM model of the crane can have the universal use. The model can be applied very easily and quickly in various simulation situations performing simple adjustment. Such situations are: a failure of any other structural element, earthquake, collision, etc. New incidental situations imply the formation of own load models.

• Contrary to high numerical vibration amplitudes in some regimes, the experimental tests at the extreme loads did not cause the dynamic instability of the structure.

• The measured stresses of the structure take place under the border of elasticity and they correspond to the numerical values. The stress obtained in the simulation can be an additional

criterion to design of a frame structure in which a local damage, caused by incident, is compensated by surrounding structural elements (redundancy).

• The deflections of the jib end obtained in the simulation correspond to the measured values and they indicate the area of higher amplitudes.

• The analyzed dynamical simulation regimes of incidental effects showed a more expressed ability to the redundancy of local structure and they did not jeopardize the global structural stability.

• The dynamic responses of the main structure elements were determined clearly by comparison of the simulation effects (regimes). The sensitivity of these elements on dynamic changes under the external perturbation effects was also determined. Thus the situation which requires the largest dynamic adjustment of the structure was found. It was an incidental situation in which the fall of load caused the interruption (fracture) of a support tie rod.

Acknowledgments

References

Cho, J.R., Han, K.C., Hwang, S.W., Cho, C.S. and Lim, O.K. (2012), "Mobile harbor: structural dynamic response of RORI crane to wave-induced rolling excitation", *Struct. Eng. Mech.*, **43**(5), 679-690.

Da Silva, J.G.S., de Lima, L.R.O., da S. Vellasco, P.C.G., de Andrade, S.A.L. and de Castro, R.A. (2008), "Nonlinear dynamic analysis of steel portal frames with semi-rigid connections", *Eng. Struct.*, **30**(9), 2566-2579.

Ibrahim, A.M., Ozturk, H. and Sabuncu, M. (2013), "Vibration analysis of cracked frame structures", *Struct. Eng. Mech.*, **45**(1), 33-52.

Isherwood, R. (2010), *Tower crane incidents worldwide*, Research report RR820, The Health and Safety Laboratory, UK.

Jovanović, M., Radoičić, G. and Marinković, D. (2012a), "Post-fracture dynamic simulation of responsible supporting structure", *Proceedings of the XI International SAUM Conference on Systems, Automatic Control and Measurements*, Niš, Serbia, November.

Jovanović, M., Radoičić, G. and Marković, D. (2012b), "Theoretical and experimental identification of the base mode of torsional vibrations of tower crane", *Proceedings of the XX International Conference MHCL'12*, Belgrade, Serbia, October.

Jovanović, M., Radoičić, G., Petrović, G. and Marković, D. (2011), "Dynamical models quality of truss supporting structures", *Facta Universitatis - Series Mech. Eng.*, **9**(2), 137-148.

Katkhuda, H.N., Dwairi, H.M. and Shatarat, N. (2010), "System identification of steel framed structures with semi-rigid connections", *Struct. Eng. Mech.*, **34**(3), 351-366.

Kettal, P. and Wiberg, N.E. (2004), "Simulation of failure of structures using dynamics and optimization techniques", *Comput. Struct.*, **82**(9-10), 815-828.

Qu, W.L., Chen, Z.H. and Xu, Y.L. (2001), "Dynamic analysis of wind-excited truss tower with friction dampers", *Comput. Struct.*, **79**(32), 2817-2831.

Radoičić, G. and Jovanović, M. (2013), "Experimental identification of overall structural damping of system", *Strojniški vestnik - J. Mech. Eng.*, **59**(4), 260-268.

Radoičić, G. and Jovanović, M. (2012), "The extreme dynamic state of main members of frame supporting structure", *Proceedings of the 23rd National Conference & 4th International Conference, Noise and Vibration*, Niš, Serbia, October.

Radoičić, G., Milić, P. and Jovanović, M. (2011), "Dynamic behavior of damaged structure of crane in the following incidental event", *Proceedings of the 7th International Conference Research and Development of Mechanical Elements and Systems*, Zlatibor, Serbia, April.

Rose, T. (2002), "An approach to properly account for structural damping, frequency-dependent stiffness/damping, and to use complex matrices in transient response", *Worldwide Aerospace Conference & Technology Showcase*, Toulouse, France, April.

Shi, G., Shi, Y., Wang, Y. and Bradford, M.A. (2008), "Numerical simulation of steel pretensioned bolted end-plate connections of different types and details", *Eng. Struct.*, **30**(10), 2677-2686.

CC